

1 **Surface EMG amplitude does not identify differences in neural drive to synergistic**  
2 **muscles**

3  
4 Eduardo Martinez-Valdes<sup>1,2,3</sup>, Francesco Negro<sup>4</sup>, Deborah Falla<sup>1</sup>, Alessandro De Nunzio<sup>1</sup>,  
5 Dario Farina<sup>5</sup>  
6

7 1- Centre of Precision Rehabilitation for Spinal Pain (CPR Spine), School of Sport,  
8 Exercise and Rehabilitation Sciences, College of Life and Environmental  
9 Sciences, University of Birmingham, Birmingham, UK

10 2- Department of Sports Medicine and Sports Orthopaedics, University of Potsdam,  
11 Potsdam, Germany

12 3- Centro de Investigación en Fisiología del Ejercicio (CIFE), Universidad Mayor,  
13 Santiago, Chile

14 4- Department of Clinical and Experimental Sciences, Università degli Studi di Brescia,  
15 Brescia, Italy

16 5- Department of Bioengineering, Imperial College London, Royal School of Mines,  
17 London, UK  
18  
19  
20

21 **Running Head:**

22 Motor unit size and EMG of synergistic muscles  
23

24 **Corresponding author:**

25 Dario Farina

26 Department of Bioengineering, Imperial College London, London, UK. Tel: +44 (0) 20 759  
27 41387, Email: d.farina@imperial.ac.uk  
28

29 **Key words**

30 Surface electromyography; Motor unit; amplitude; motor unit action potential; high-density  
31 surface EMG: synergistic muscles  
32  
33  
34

35 **ABSTRACT**

36

37 Surface electromyographic (EMG) signal amplitude is typically used to compare the neural  
38 drive to muscles. We experimentally investigated this association by studying the motor unit  
39 (MU) behavior and action potentials in the vastus medialis (VM) and vastus lateralis (VL)  
40 muscles. Eighteen participants performed isometric knee extensions at four target torques [10,  
41 30, 50 and 70% of the maximum torque (MVC)] while high-density EMG signals were  
42 recorded from the VM and VL. The absolute EMG amplitude was greater for VM than VL  
43 ( $p < 0.001$ ) while the EMG amplitude normalized with respect to MVC was greater for VL than  
44 VM ( $p < 0.04$ ). Because differences in EMG amplitude can be due to both differences in the  
45 neural drive and in the size of the MU action potentials, we indirectly inferred the neural drives  
46 received by the two muscles by estimating the synaptic inputs received by the corresponding  
47 motor neuron pools. For this purpose, we analyzed the increase in discharge rate from  
48 recruitment to target torque for motor units matched by recruitment threshold in the two  
49 muscles. This analysis indicated that the two muscles received similar levels of neural drive.  
50 Nonetheless, the size of the MU action potentials was greater for VM than VL ( $p < 0.001$ ) and  
51 this difference explained most of the differences in EMG amplitude between the two muscles  
52 (~63% of explained variance). These results indicate that EMG amplitude, even following  
53 normalization, does not reflect the neural drive to synergistic muscles. Moreover, absolute  
54 EMG amplitude is mainly explained by the size of MU action potentials.

55

56 **New and Noteworthy**

57 EMG amplitude is widely used to indirectly compare the strength of neural drive received by  
58 synergistic muscles. However, there are no studies validating this approach with motor unit  
59 data. Here, we compared between-muscles differences in surface EMG amplitude and motor  
60 unit behavior. The results clarify the limitations of surface EMG to interpret differences in  
61 neural drive between muscles.

62

63

64

65

66

67

68

## 69 INTRODUCTION

70

71 Surface electromyography (EMG) amplitude depends on the level of muscle activation  
72 (number of muscle fiber action potentials) and it is typically used to infer the strength of neural  
73 drive (number of motor neuron action potentials) received by muscles (6). Changes in the  
74 relative activations of synergistic muscles are believed to be associated to the development of  
75 musculoskeletal disorders (19). For example, researchers argue that pathologies such as  
76 patellofemoral joint pain and Achilles tendinopathy might occur due to misbalanced activation  
77 of the vasti and calf muscles, respectively (17, 19). For patellofemoral joint pain, it is assumed  
78 that a greater activation of the vastus lateralis (VL) compared to the vastus medialis (VM)  
79 muscle induces a lateral shift of the patella, leading to misalignment of the patellofemoral joint  
80 (17, 19). Although these explanations seem plausible, there is still no consensus in the literature  
81 (7, 31), mainly because of limitations of surface EMG amplitude in measuring the neural drive  
82 (6). While normalization of EMG amplitude with respect to its value during a maximal  
83 voluntary contraction (MVC) may increase reliability when comparing between subjects (4),  
84 normalization may cancel out changes in muscle activation following, e.g., training  
85 interventions. It has been recently shown that high-density EMG (HDEMG) systems provide  
86 more reliable estimates of signal amplitude without the need for normalization (14, 34). This  
87 is possible due to the large number of observation sites (tens of electrodes) over the muscle  
88 belly that compensate for the variability of EMG with electrode location. However, the use of  
89 several electrodes does not solve the problem of comparing between muscles and subjects.

90 In addition to the neural drive to the muscle, EMG amplitude estimates are influenced by  
91 several other factors, such as muscle architecture, geometry, EMG crosstalk, and subcutaneous  
92 tissue thickness (11). Although normalization could help to improve between-muscle  
93 amplitude estimates, it is still not known if such measures really reflect differences in neural  
94 drive to the muscles. The direct way to access the neural drive to muscles is by motor unit  
95 recordings. Recent research has shown the possibility to identify large populations of motor  
96 units non-invasively, with HDEMG (25, 27). However, even sampling relatively large numbers  
97 of motor units, it is not possible to directly compare the strength of the neural drive to different  
98 muscles since the decomposition cannot identify the entire pool of active motor units. Rather,  
99 the number of decomposed motor units varies among muscles, with a weak relation with the  
100 actual number of active units. For this reason, in this study we propose a way to indirectly infer  
101 differences in neural drive between muscles by estimating the synaptic inputs received by their  
102 motor neuron pools. Assuming similar intrinsic properties of the motor neurons between the

103 muscles, we analyzed the increase in discharge rate from recruitment to target torque for motor  
104 units matched by recruitment threshold in the two muscles. Differences in the increase of  
105 discharge rate for motor units with the same recruitment thresholds would indicate differences  
106 in synaptic input received by the corresponding motor neurons and therefore differences in the  
107 generated neural drive to the muscles. In addition, we estimated the amplitude of the individual  
108 motor unit action potentials to examine the associations between interference EMG amplitude  
109 and either motor unit action potential size or neural drive. Therefore, the aim of the study was  
110 to assess the strengths of neural drives received by VM and VL muscles and investigate their  
111 relations with EMG amplitude. We hypothesized that differences in EMG amplitude between  
112 VM and VL muscles would be largely determined by the size of the motor unit action potentials  
113 (MUAPs) rather than differences in neural drive to the two muscles, and that normalization  
114 would not completely compensate for this influence.

115

## 116 **MATERIALS AND METHODS**

### 117 Participants

118 Eighteen healthy and physically active men (mean (SD) age: 29 (3) years, height: 178 (6) cm,  
119 mass: 79 (9) kg) were recruited. None of the participants reported any history of neuromuscular  
120 disorders or previous lower limb surgery. Subjects were asked to avoid any strenuous activity  
121 24 h prior to the measurements. The ethics committee of the Universität Potsdam approved the  
122 study (approval number 26/2015), in accordance with the declaration of Helsinki (2004). All  
123 participants gave written, informed consent.

### 124 Experimental protocol

125 The participants performed submaximal and maximal knee extension contractions on an  
126 isokinetic dynamometer (CON-TREX MJ, PHYSIOMED, Regensdorf, Switzerland). The  
127 isometric knee extensions were exerted with the knee flexed to 90°. After placement of the  
128 surface EMG electrodes (see Data acquisition), subjects performed three maximal voluntary  
129 contractions (MVC) of knee extension each over a period of 5 s. Each of these trials was  
130 separated by 2 min of rest. The highest MVC value served as a reference to define the  
131 submaximal torque levels. After 5 min of rest, and following familiarization trials at low torque  
132 levels (10 and 30% MVC), subjects performed submaximal isometric knee extension  
133 contractions at 10, 30, 50 and 70% MVC in random order. Contractions at 10 and 30% MVC  
134 were maintained for 20 s, while the contractions at 50 and 70% MVC were sustained for 15  
135 and 10 s respectively. In each trial, the participants received visual feedback of the torque  
136 applied by the leg to the dynamometer, which was displayed as a trapezoid (5 s ramps with

137 hold-phase durations as specified above). Each contraction level was performed twice with a  
138 rest of 2 min following each contraction.

### 139 Data Acquisition

140 The surface EMG signals of VM and VL were recorded in monopolar derivation with a two-  
141 dimensional adhesive grid (SPES Medica, Salerno, Italy) of  $13 \times 5$  equally spaced electrodes  
142 (1 mm diameter, inter-electrode distance of 8 mm). EMG signals were initially recorded during  
143 a brief voluntary contraction during which a linear non-adhesive dry electrode array of 8 silver-  
144 bar electrodes (1-mm diameter, 5-mm length, 5 mm interelectrode distance; SA 8/5, OT  
145 Bioelettronica, Torino, Italy) was moved over the skin to detect the location of the innervation  
146 zone and tendon regions (23). After the skin was shaved and cleansed with abrasion and water,  
147 the electrode cavities of the grids were filled with conductive paste (SPES Medica, Salerno,  
148 Italy). Grids were positioned between the proximal and distal tendons of the VM and VL  
149 muscles with the electrode columns (comprising 13 electrodes) oriented along the muscle  
150 fibers. Therefore, the VM grid was positioned  $\sim 50^\circ$  with respect to a line between the anterior  
151 superior iliac spine and the medial side of the patella while the VL grid was positioned  $\sim 30^\circ$   
152 with respect to a line between the anterior superior iliac spine and the lateral side of the patella  
153 ((1, 22, 24, 25) (Figure 1). Reference electrodes were positioned over the malleoli and patella  
154 of the dominant leg.

155 EMG and torque signals were sampled at 2048 Hz and converted to digital data by a 12-bit  
156 analogue to digital converter (EMG-USB 2, 256-channel EMG amplifier, OT Bioelettronica,  
157 Torino, Italy, 3dB, bandwidth 10-500 Hz). EMG signals were amplified by a factor of 2000,  
158 1000, 500, 500 and 500 for the 10, 30, 50, 70 and 100% MVC contractions, respectively. Data  
159 were analysed offline using Matlab (The Mathworks Inc., Natick, Massachusetts, USA). The  
160 64-monopolar EMG channels were re-referenced offline to form 59 bipolar channels as the  
161 differences between adjacent electrodes in the direction of the muscle fibers.

### 162 Signal analysis

163 *Motor unit analysis.* The EMG signals recorded during the submaximal isometric contractions  
164 (from 10 to 70% MVC) were decomposed offline with a method that has undergone extensive  
165 validation (28). The accuracy of the decomposition was tested with the silhouette measure,  
166 which was set to  $\geq 0.90$  (28). The signals were decomposed throughout the whole duration of  
167 the submaximal contractions and the discharge times of the identified motor units were  
168 converted into binary spike trains. The mean discharge rate and discharge rate variability  
169 (coefficient of variation of the inter-spike-interval, CoVisi), were calculated during the stable  
170 plateau torque region. Discharge rate at recruitment was calculated using the first six discharges

171 of the motor units (9). The motor unit recruitment threshold was defined as the knee extension  
172 torque (%MVC) at the time when the motor unit began discharging action potentials.  
173 Discharges that were separated from the next by  $<33.3$  ms or  $>200$  ms (30 and 5 Hz,  
174 respectively) were discarded from the mean discharge rate and CoVisi calculation since such  
175 discharges are usually considered decomposition errors (24). Motor unit conduction velocity  
176 (MUCV) was measured from a minimum of three to a maximum of nine double-differential  
177 channels (manual selection) (25). Channels that had the clearest propagation of MUAPs, with  
178 the highest amplitude in the columns of the grid and a coefficient of correlation between  
179 channels  $\geq 0.9$ , were selected for further analysis. Finally, the amplitude of the MUAPs was  
180 calculated as the MUAP RMS averaged over all channels of the grid (MURMS). VM and VL  
181 motor units were matched by their recruitment threshold with a tolerance of  $\pm 0.5\%$  MVC. The  
182 matched motor units were then grouped in four classes, according to their recruitment  
183 thresholds ([0-10] % MVC, [10-30] % MVC, [30-50] % MVC, [50-70] % MVC).  
184 The discharge rate of motor units with the same recruitment thresholds (i.e., with a difference  
185 in threshold  $<0.5\%$  MVC) in the two muscles was used as a measure to compare the synaptic  
186 inputs received by the pools of motor neurons. This measure corresponds to the increase in  
187 discharge rate from recruitment to the target torque relative to the increase in torque from the  
188 recruitment threshold [target torque (10, 30, 50 and 70% MVC) – recruitment threshold  
189 torque]. A difference in the relative rate of increase in discharge rate between motor units in  
190 the two muscles indicates differences in synaptic input received by the motor neuron pools of  
191 the two muscles. It was then assumed that the neural drive to the muscles depended on the  
192 synaptic input.

193 *Interference EMG.* The root mean square values (RMS) obtained from submaximal and  
194 maximal contractions, were averaged over all channels of the electrode grid (22). During the  
195 submaximal isometric contractions, the RMS was computed from the HDEMG signals in  
196 intervals of 1 s. These values were extracted from the stable-torque region of the contractions  
197 (e.g., hold-phase of 15 seconds at 50% MVC). RMSs of the maximal (MVC) contractions were  
198 analyzed in a time window of 250 ms centered at the peak EMG activity (22). The average  
199 conduction velocity (referred in the following as muscle fiber conduction velocity) was  
200 calculated from the interference EMG in double differential derivations obtained along the  
201 fiber direction (columns of the grid). In order to maximize the accuracy of muscle fiber  
202 conduction velocity estimates, three contiguous columns with four to six channels with the  
203 highest cross-correlation in propagation were selected (10). Muscle fiber conduction velocity

204 estimation was obtained with a multichannel maximum-likelihood algorithm that was  
205 previously shown to provide accurate estimates (standard deviation <0.1 ms) (13).

206 *Amplitude normalization.* Both absolute RMS and MURMS were normalized to the RMS value  
207 obtained during the MVC in order to analyze the effects of normalization on submaximal RMS  
208 amplitude of the interference EMG (absolute RMS) as well as on MURMS between muscles.

209

## 210 Statistical Analysis

211 The Shapiro-Wilk test was used to check the normality of all variables. Sphericity was checked  
212 by the Mauchly's test and if violated, the Greenhouse-Geisser correction was applied to the  
213 degrees of freedom. Statistical significance was set at  $p < 0.05$ . Results are expressed as mean  
214 and standard deviation (SD).

215 EMG (absolute RMS, normalized RMS and muscle fiber conduction velocity) and motor unit  
216 variables (MURMS, discharge rate, CoVisi, motor unit conduction velocity and normalized  
217 MURMS) were compared between muscles at each torque level with a two-way repeated  
218 measures analysis of variance (ANOVA) with factors muscle (VM and VL) and torque (10,  
219 30, 50 and 70% MVC). When the repeated measures ANOVA was significant, pairwise  
220 comparisons were performed with a Student-Newman-Keuls (SNK) post-hoc test. Linear  
221 regression was used to characterize the association for each motor unit between the differences  
222 in discharge rate at the target torque (mean discharge rate at 10, 30, 50 and 70% MVC) and at  
223 recruitment (calculated from the first 6 motor unit discharges) and between the target torque  
224 (10, 30, 50 and 70% MVC) and motor unit recruitment threshold. The slopes of these linear  
225 regressions were compared between the two muscles by analysis of covariance (ANCOVA)  
226 (35). The same analysis was applied to VM and VL MURMS vs. recruitment threshold.

227 Finally, a multiple linear regression (stepwise) analysis was performed on EMG/motor unit  
228 parameters to identify the variables that predicted the differences between VM and VL absolute  
229 RMS. Therefore, the percent (%) difference in absolute RMS between VM and VL was used  
230 as the predictor variable and the % differences in MU behavior/properties were regarded as  
231 independent variables. Each torque level was analyzed independently (e.g. absolute RMS %  
232 difference between VM and VL at 30% MVC was compared with motor unit variables obtained  
233 at the same torque level). The partial eta-squared ( $\eta^2$ ) for ANOVA was used to examine the  
234 effect size of the differences between EMG and motor unit parameters between muscles. A  $\eta^2$   
235 less than 0.06 was classified as "small", 0.07-0.14 as "moderate", and greater than 0.14 as  
236 "large" (5).

237

## 238 RESULTS

239

### 240 Interference EMG

241 Absolute RMS (Figure 2a) was significantly greater for VM than VL at 30, 50 and 70% MVC  
242 (interaction: muscle-torque,  $p<0.0001$ ,  $\eta^2=0.79$ ). However, muscle fiber conduction velocity  
243 (Figure 2b) was similar for the two muscles (interaction: muscle-torque,  $p=0.96$ ,  $\eta^2=0.019$ ).

244

### 245 Decomposed motor unit populations

246 The average number of motor units accurately identified (with a  $SIL\geq 0.90$ ) per subject at each  
247 torque level was 8 (0.7) and 7 (1.2) in VM and VL, respectively.

248 According to their recruitment threshold, 340 motor units were matched between VM and VL.  
249 Per subject, an average of 6.2 (3.0), 5.0 (2.5), 5.7 (2.8) and 3.3 (2.0) motor units were matched  
250 between VM and VL at 10, 30, 50 and 70% MVC, respectively. The average recruitment  
251 threshold of the matched motor units at 10, 30, 50 and 70% MVC was 7.5, 23.3, 38.2 and  
252 56.2% MVC, respectively. Figure 3 shows the histograms of the number of matched motor  
253 units according to their recruitment thresholds.

254

### 255 Discharge rate and discharge rate variability

256 The mean motor unit discharge rate (at target torque) of VM was greater than for VL motor  
257 units as revealed by a significant effect of muscle ( $p=0.009$ ,  $\eta^2=0.38$ ) (Figure 4). However,  
258 the regression lines of delta discharge rate [mean discharge rate at target torque – discharge  
259 rate at recruitment] vs. delta torque [target torque – recruitment threshold] were not different  
260 between muscles (slope of the regression lines,  $p>0.35$ , intercepts,  $p>0.08$ ) at all target torques  
261 (10, 30, 50 and 70% MVC) (Figure 5). Finally, there was no difference in discharge rate  
262 variability between muscles as CoVisi (Figure 6) remained similar at all torque levels  
263 (interaction: muscle-torque,  $p=0.4$ ,  $\eta^2=0.07$ ).

264

### 265 Size and conduction velocity of MUAPs

266 MURMS (Figure 7a) was significantly greater for VM than VL at 30, 50 and 70% MVC  
267 (interaction: muscle-torque,  $p<0.0001$ ,  $\eta^2=0.57$ ). Moreover, MURMS increased at a greater  
268 rate with recruitment threshold for VM than for VL ( $p<0.0001$ , Figure 7b). Motor unit  
269 conduction velocity (Figure 8) was significantly higher at 70% MVC for VM than VL  
270 (interaction: muscle-torque,  $p=0.023$ ,  $\eta^2=0.46$ ).

271



## 272 Multiple linear regression

273 Motor unit variables that significantly differed between muscles were entered into the multiple  
274 linear regression analysis to explain the differences in absolute EMG amplitude between  
275 muscles. Therefore, the difference (%) in VM-VL MURMS, discharge rate, and motor unit  
276 conduction velocity were regarded as independent variables. Table 1 reports the results of the  
277 multiple regression. At 10% MVC, only MURMS was entered in the model, explaining 71%  
278 of the variance for the difference (%) in VM-VL absolute RMS. At 30%, both MURMS and  
279 discharge rate entered in the model, however MURMS explained most of the variance (53%  
280 MURMS vs. 13.2% for discharge rate). Similar results were obtained at 50% MVC where  
281 MURMS explained 72% of the difference between VM-VL absolute RMS, with discharge rate  
282 only explaining 7.7% of the variance. Finally, at 70% MVC, only MURMS was entered in the  
283 model, explaining 57% of the %difference in VM-VL absolute RMS.

284

## 285 Normalized amplitude

286 Normalized RMS (Figure 9) showed systematically higher values for VL across all torque  
287 levels (effect: muscle,  $p=0.039$ ,  $\eta^2=0.23$ ). Conversely, normalized MURMS did not show any  
288 difference between muscles at any torque level (effect: muscle,  $p=0.46$ ,  $\eta^2=0.04$ , interaction:  
289 torque-muscle,  $p=0.12$ ,  $\eta^2=0.11$ ).

290

## 291 **DISCUSSION**

292

293 This study shows that differences in EMG amplitude between synergistic muscles are mostly  
294 explained by differences in MUAP size (MURMS), with little influence of other motor unit  
295 properties. Moreover, EMG normalization does not provide clear explanation of differences in  
296 muscle activation between the vasti. The observed differences in EMG amplitude between  
297 muscles (in absolute values or normalized) contrasted with the similar neural drive estimated  
298 for VM and VL. Taken together, the results suggest that EMG amplitude (in absolute values or  
299 normalized) should not be used to infer differences in neural drive between synergistic muscles.

300

## 301 Neural drive to VM and VL muscles

302 Due to current limitations in EMG decomposition, it is not possible to identify the full  
303 populations of active motor units. For this reason, the neural drives cannot be directly compared  
304 between muscles. We compensated for this limitation by an indirect assessment of the strength  
305 of the neural drive. Matching synergistic muscles motor units by recruitment threshold allows

306 a direct comparison of motor unit discharge rates across muscles. Because the discharge rate  
307 depends on the torque relative to the recruitment threshold, we focused on the rate of change  
308 in discharge rate (mean discharge rate at target torque – discharge rate at recruitment) with  
309 respect to the difference between exerted torque (10, 30, 50 or 70% MVC) and recruitment  
310 threshold across the decomposed motor unit populations. This analysis provides an estimate of  
311 the synaptic input received by the motor neuron pools of VM and VL, since discharge rates  
312 indicate the nonlinear transformation of synaptic inputs into motor neuron outputs (20). This  
313 approach indicated a similar change in motor unit discharge rate with torque (figure 5) despite  
314 a difference in absolute discharge rates that can be due to the random sampling of motor units  
315 in the two muscles (Figure 4). This suggests that the net excitatory synaptic input to the pool  
316 of motor neurons of the vasti was similar. Assuming that the intrinsic properties of the motor  
317 neuron pools in the two muscles were similar, this observation was interpreted as reflecting  
318 similar drives from the motor neurons to the muscle units. This conclusion is in agreement with  
319 a previous study that showed that VM and VL share most of their synaptic input (21).  
320 We also did not observe differences in discharge rate variability (CoVisi) between the two  
321 muscles (Figure 6), in agreement with previous results (34). The present results show that,  
322 despite a difference in mean absolute discharge rates between motor units of the VM and VL,  
323 the two muscles did receive similar strengths of neural drives. Differences in VM and VL  
324 surface EMG amplitude therefore do not reflect differences in the neural drive between the  
325 vasti, as also confirmed by the multiple regression analysis.

326

327 EMG amplitude and muscle fiber conduction velocity

328 Surface EMG amplitude is commonly used to infer the magnitude of the neural drive to  
329 muscles. However, EMG amplitude depends on both motor unit behavior (recruitment,  
330 discharge rate and discharge rate variability) and muscle fiber properties (MUAP size and  
331 conduction velocity) (11, 12). In this study, despite similar neural drives to the VM and VL,  
332 the EMG amplitude for VM was significantly greater than for VL for torques in the range 30%-  
333 70% MVC (Figure 7). These results are consistent with other reports on absolute EMG  
334 amplitude for these two muscles (15, 22, 34). EMG amplitude is influenced by muscle's  
335 geometry, architecture, crosstalk and subcutaneous tissue thickness (11, 29). Since the  
336 observed differences in EMG amplitude between muscles did not correspond to differences in  
337 neural drive, they are mainly explained by these anatomical factors, as confirmed by the  
338 differences in MUAP sizes. Although previous research has reported similar subcutaneous  
339 tissue thickness for the distal VM and VL (3), it has also been shown that the distal VM has a

340 larger cross sectional area and greater fascicle angle compared to the distal VL (2). Indeed,  
341 recent research has shown that differences in muscle architecture can influence EMG  
342 amplitude, even when the muscle is activated at a similar intensity (32).

343 Muscle fiber conduction velocity estimated from the interference EMG was similar between  
344 the vasti, in agreement with previous studies (3). However, motor unit conduction velocity  
345 differed between muscles. Muscle fiber conduction velocity is associated to fiber diameter (16)  
346 but also depends on the level of muscle acidosis (30), temperature (8), muscle fatigability (23),  
347 subcutaneous tissue thickness (33), exercise training (25, 33), discharge rate (26). Because of  
348 these factors of influence, the relation between average and motor unit muscle fiber conduction  
349 velocity is not exactly linear.

350

#### 351 EMG amplitude and MUAP size

352 As for absolute EMG amplitude, the size of MUAPs was significantly greater for VM in the  
353 range of torques above or equal to 30% MVC. Moreover, MURMS increased at a faster rate  
354 with recruitment threshold for VM than VL (Figure 7). This is consistent with a recent report  
355 comparing VM and VL MUAP peak-to-peak amplitude (24). As for EMG amplitude, MURMS  
356 is also influenced by muscle's geometry, architecture and subcutaneous tissue thickness (11,  
357 29); therefore it is not surprising to find similar results for absolute RMS and MURMS.  
358 Accordingly, results from the multiple linear regression (Table 1) showed that most of the  
359 variance of the difference between absolute RMS of VM and VL was explained by MURMS.  
360 This result directly indicates that the neural drive has a relatively small influence on EMG  
361 amplitude with respect to the MUAP waveforms.

362

#### 363 Amplitude normalization

364 Since a vast number of studies apply normalization of the surface EMG prior to comparing  
365 levels of muscle activations (4, 17), we analyzed the effect of normalization of both EMG  
366 amplitude and MUAP size with respect to MVC. Even though normalization decreased the  
367 VM/VL activation ratio and cancelled out the differences in MUAP size between muscles,  
368 normalized EMG amplitude was greater for VL compared to VM that is contrary to the result  
369 without normalization. This result does not correspond to the estimated similar neural drive to  
370 the two muscles (figure 5) and explains the divergent results across studies on normalized  
371 activations of the VM and VL in healthy subjects (31) and patients with musculoskeletal  
372 disorders (e.g. patellofemoral pain syndrome) (18). Taken together, our findings suggest that

373 neither absolute nor normalized EMG amplitude (even when recorded from HDEMG  
374 electrodes) are appropriate for inferring differences in neural drive between muscles.

375

376 Conclusion

377 The difference in surface EMG amplitude between VM and VL muscles was mostly explained  
378 by differences in MUAP size, with little effect of motor unit properties associated to the neural  
379 drive to muscles. EMG amplitude is therefore mainly determined by peripheral properties  
380 rather than by the neural activation. Normalization of the EMG compensates for the differences  
381 in MUAP sizes but is still a poor determinant of neural activation.

382

### 383 REFERENCES

384

- 385 1. **Barbero M, Merletti R, and Rainoldi A.** *Atlas of muscle innervation zones :  
386 understanding surface electromyography and its applications.* Milan ; New York: Springer,  
387 2012, p. 131-132.
- 388 2. **Blazevich AJ, Gill ND, and Zhou S.** Intra- and intermuscular variation in human  
389 quadriceps femoris architecture assessed in vivo. *J Anat* 209: 289-310, 2006.
- 390 3. **Boccia G, Dardanello D, Beretta-Piccoli M, Cescon C, Coratella G, Rinaldo N, Barbero  
391 M, Lanza M, Schena F, and Rainoldi A.** Muscle fiber conduction velocity and fractal dimension  
392 of EMG during fatiguing contraction of young and elderly active men. *Physiol Meas* 37: 162-  
393 174, 2016.
- 394 4. **Burden A.** How should we normalize electromyograms obtained from healthy  
395 participants? What we have learned from over 25 years of research. *J Electromyogr Kinesiol*  
396 20: 1023-1035, 2010.
- 397 5. **Cohen J.** *Statistical power analysis for the behavioral sciences.* Hillsdale, N.J.: L.  
398 Erlbaum Associates, 1988, p. xxi, 567 p.
- 399 6. **Dideriksen JL, Enoka RM, and Farina D.** Neuromuscular adjustments that constrain  
400 submaximal EMG amplitude at task failure of sustained isometric contractions. *J Appl Physiol*  
401 (1985) 111: 485-494, 2011.
- 402 7. **Fagan V, and Delahunt E.** Patellofemoral pain syndrome: a review on the associated  
403 neuromuscular deficits and current treatment options. *Br J Sports Med* 42: 789-795, 2008.
- 404 8. **Farina D, Arendt-Nielsen L, and Graven-Nielsen T.** Effect of temperature on spike-  
405 triggered average torque and electrophysiological properties of low-threshold motor units. *J*  
406 *Appl Physiol (1985)* 99: 197-203, 2005.
- 407 9. **Farina D, Holobar A, Gazzoni M, Zazula D, Merletti R, and Enoka RM.** Adjustments  
408 differ among low-threshold motor units during intermittent, isometric contractions. *J*  
409 *Neurophysiol* 101: 350-359, 2009.
- 410 10. **Farina D, and Merletti R.** Estimation of average muscle fiber conduction velocity from  
411 two-dimensional surface EMG recordings. *J Neurosci Methods* 134: 199-208, 2004.
- 412 11. **Farina D, Merletti R, and Enoka RM.** The extraction of neural strategies from the  
413 surface EMG. *J Appl Physiol (1985)* 96: 1486-1495, 2004.
- 414 12. **Farina D, Merletti R, and Enoka RM.** The Extraction of Neural Strategies from the  
415 Surface Emg: An Update. *J Appl Physiol (1985)* jap 00162 02014, 2014.

- 416 13. **Farina D, Muhammad W, Fortunato E, Meste O, Merletti R, and Rix H.** Estimation of  
417 single motor unit conduction velocity from surface electromyogram signals detected with  
418 linear electrode arrays. *Med Biol Eng Comput* 39: 225-236, 2001.
- 419 14. **Gallina A, Pollock CL, Vieira TM, Ivanova TD, and Garland SJ.** Between-day reliability  
420 of triceps surae responses to standing perturbations in people post-stroke and healthy  
421 controls: A high-density surface EMG investigation. *Gait Posture* 44: 103-109, 2016.
- 422 15. **Hedayatpour N, Arendt-Nielsen L, and Farina D.** Non-uniform electromyographic  
423 activity during fatigue and recovery of the vastus medialis and lateralis muscles. *J*  
424 *Electromyogr Kinesiol* 18: 390-396, 2008.
- 425 16. **Houtman CJ, Stegeman DF, Van Dijk JP, and Zwarts MJ.** Changes in muscle fiber  
426 conduction velocity indicate recruitment of distinct motor unit populations. *J Appl Physiol*  
427 (1985) 95: 1045-1054, 2003.
- 428 17. **Hug F, Goupille C, Baum D, Raiteri BJ, Hodges PW, and Tucker K.** Nature of the  
429 coupling between neural drive and force-generating capacity in the human quadriceps  
430 muscle. *Proc Biol Sci* 282: 2015.
- 431 18. **Hug F, Hodges PW, and Tucker K.** Muscle Force Cannot Be Directly Inferred From  
432 Muscle Activation: Illustrated by the Proposed Imbalance of Force Between the Vastus  
433 Medialis and Vastus Lateralis in People With Patellofemoral Pain. *J Orthop Sports Phys Ther*  
434 45: 360-365, 2015.
- 435 19. **Hug F, and Tucker K.** Muscle Coordination and the Development of Musculoskeletal  
436 Disorders. *Exerc Sport Sci Rev* 45: 201-208, 2017.
- 437 20. **Johnson MD, Thompson CK, Tysseling VM, Powers RK, and Heckman CJ.** The  
438 potential for understanding the synaptic organization of human motor commands via the  
439 firing patterns of motoneurons. *J Neurophysiol* 118: 520-531, 2017.
- 440 21. **Laine CM, Martinez-Valdes E, Falla D, Mayer F, and Farina D.** Motor Neuron Pools of  
441 Synergistic Thigh Muscles Share Most of Their Synaptic Input. *J Neurosci* 35: 12207-12216,  
442 2015.
- 443 22. **Martinez-Valdes E, Falla D, Negro F, Mayer F, and Farina D.** Differential Motor Unit  
444 Changes after Endurance or High-Intensity Interval Training. *Med Sci Sports Exerc* 49: 1126-  
445 1136, 2017.
- 446 23. **Martinez-Valdes E, Guzman-Venegas RA, Silvestre RA, Macdonald JH, Falla D,**  
447 **Araneda OF, and Haichelis D.** Electromyographic adjustments during continuous and  
448 intermittent incremental fatiguing cycling. *Scand J Med Sci Sports* 26: 1273-1282, 2016.
- 449 24. **Martinez-Valdes E, Laine CM, Falla D, Mayer F, and Farina D.** High-density surface  
450 electromyography provides reliable estimates of motor unit behavior. *Clin Neurophysiol* 127:  
451 2534-2541, 2016.
- 452 25. **Martinez-Valdes E, Negro F, Laine CM, Falla D, Mayer F, and Farina D.** Tracking motor  
453 units longitudinally across experimental sessions with high-density surface  
454 electromyography. *J Physiol* 595: 1479-1496, 2017.
- 455 26. **McGill KC, and Lateva ZC.** History dependence of human muscle-fiber conduction  
456 velocity during voluntary isometric contractions. *J Appl Physiol* (1985) 111: 630-641, 2011.
- 457 27. **Muceli S, Poppendieck W, Negro F, Yoshida K, Hoffmann KP, Butler JE, Gandevia SC,**  
458 **and Farina D.** Accurate and representative decoding of the neural drive to muscles in humans  
459 with multi-channel intramuscular thin-film electrodes. *J Physiol* 593: 3789-3804, 2015.
- 460 28. **Negro F, Muceli S, Castronovo AM, Holobar A, and Farina D.** Multi-channel  
461 intramuscular and surface EMG decomposition by convolutive blind source separation. *J*  
462 *Neural Eng* 13: 026027, 2016.

- 463 29. **Rainoldi A, Nazzaro M, Merletti R, Farina D, Caruso I, and Gaudenti S.** Geometrical  
464 factors in surface EMG of the vastus medialis and lateralis muscles. *J Electromyogr Kinesiol*  
465 10: 327-336, 2000.
- 466 30. **Schmitz JP, van Dijk JP, Hilbers PA, Nicolay K, Jeneson JA, and Stegeman DF.**  
467 Unchanged muscle fiber conduction velocity relates to mild acidosis during exhaustive  
468 bicycling. *Eur J Appl Physiol* 112: 1593-1602, 2012.
- 469 31. **Smith TO, Bowyer D, Dixon J, Stephenson R, Chester R, and Donell ST.** Can vastus  
470 medialis oblique be preferentially activated? A systematic review of electromyographic  
471 studies. *Physiother Theory Pract* 25: 69-98, 2009.
- 472 32. **Vieira TM, Bisi MC, Stagni R, and Botter A.** Changes in tibialis anterior architecture  
473 affect the amplitude of surface electromyograms. *J Neuroeng Rehabil* 14: 81, 2017.
- 474 33. **Vila-Cha C, Falla D, Correia MV, and Farina D.** Adjustments in motor unit properties  
475 during fatiguing contractions after training. *Med Sci Sports Exerc* 44: 616-624, 2012.
- 476 34. **Vila-Cha C, Falla D, and Farina D.** Motor unit behavior during submaximal contractions  
477 following six weeks of either endurance or strength training. *J Appl Physiol (1985)* 109: 1455-  
478 1466, 2010.
- 479 35. **Zar JH.** *Biostatistical analysis*. Upper Saddle River, N.J.: Prentice-Hall/Pearson, 2010,  
480 p. 944.

481

## 482 **Acknowledgements**

483 Francesco Negro has received funding from the European Union's Horizon 2020 research and  
484 innovation programme under the Marie Skłodowska-Curie grant agreement No 702491  
485 (NeuralCon).

486

487

488

489

490

491

492

493

494

495

496

497

498

499

500

501

502 **Figure captions**

503

504 Figure 1. Placement of the HDEMG electrodes. Vastus medialis (VM) electrode grid was  
505 placed  $\sim 50^\circ$  with respect to a line between the anterior superior iliac spine and the medial side  
506 of the patella (dashed lines, left) while the VL grid was positioned  $\sim 30^\circ$  with respect to a line  
507 between the anterior superior iliac spine and the lateral side of the patella (dashed lines, right).

508

509 Figure 2. Interference EMG parameters [mean (SD)] for vastus medialis (VM, white dots) and  
510 vastus lateralis (VL, black dots) at 10, 30, 50 and 70% of the maximum voluntary contraction  
511 torque (MVC). A) Absolute root mean square (ABS RMS). B) Muscle fiber conduction  
512 velocity. Presented values were averaged for each subject and presented at each submaximal  
513 target torque. \*  $P < 0.001$ .

514

515 Figure 3. Two subsets of motor units identified from the vastus medialis and lateralis muscles  
516 were matched for recruitment threshold. The histograms of the motor unit recruitment  
517 thresholds in these subsets are shown for the vastus medialis (left) and vastus lateralis (right)  
518 motor units.

519

520 Figure 4. Motor unit (MU) average discharge rate (target torque discharge rate) calculated from  
521 recruitment-threshold matched MUs from vastus medialis (VM, white dots) and vastus lateralis  
522 (VL, black dots) at 10, 30, 50 and 70% of the maximum voluntary contraction torque (MVC).  
523 MU discharge rate values [mean (SD)] were averaged for each subject and presented at each  
524 submaximal target torque (10, 30, 50 and 70% MVC), # main effect of muscle  $P = 0.009$ .

525

526 Figure 5. Linear regression analysis of the difference between VM and VL mean discharge rate  
527 at target torque and discharge rate at recruitment (Y-axis) and the difference between target  
528 torque (10, 30, 50 and 70% MVC) and MU recruitment threshold (X-axis) at 10% (upper left),  
529 30% (upper right), 50% (lower left) and 70% (lower right) of the MVC torque. Linear  
530 regression equations are shown in the figure. All regression lines had positive slopes ( $P < 0.03$ )  
531 and their  $R^2$  values were 0.1 and 0.15 (10% MVC), 0.16 and 0.08 (30% MVC), 0.05 and 0.05  
532 (50% MVC), and 0.17 and 0.14 (70% MVC) for VM and VL respectively. None of the  
533 regression lines (slopes and intercepts) differed significantly between muscles ( $p > 0.09$ ). DR,  
534 discharge rate.

535

536 Figure 6. Motor unit (MU) coefficient of variation of the inter-spike interval (CoVisi)  
537 calculated from recruitment-threshold matched MUs from vastus medialis (VM, white dots)  
538 and vastus lateralis (VL, black dots) at 10, 30, 50 and 70% of the maximum voluntary  
539 contraction torque (MVC). Presented values were averaged for each subject and presented at  
540 each submaximal target torque.

541

542 Figure 7. Motor unit (MU) root mean square amplitude (MURMS) [mean (SD)] extracted from  
543 recruitment-threshold matched MUs from vastus medialis (VM, white dots) and vastus lateralis  
544 (VL, black dots) at 10, 30, 50 and 70% of the maximum voluntary contraction torque (MVC).  
545 A) MURMS values [mean (SD)] were averaged for each subject and presented at each  
546 submaximal target torque (10, 30, 50 and 70% MVC), \*  $P < 0.01$ . B) VM and VL MURMS vs.  
547 recruitment threshold regression lines. Both lines increased significantly with torque  
548 ( $P < 0.0001$ ) and displayed significantly different slopes ( $P < 0.0001$ );  $R^2$  values are shown in the  
549 figure.

550

551 Figure 8. Motor unit (MU) conduction velocity [mean (SD)] extracted from recruitment-  
552 threshold matched MUs from vastus medialis (VM, white dots) and vastus lateralis (VL, black  
553 dots) at 10, 30, 50 and 70% of the maximum voluntary contraction torque (MVC). Presented  
554 values were averaged for each subject and presented at each submaximal target torque. \*  
555  $P < 0.01$ .

556

557 Figure 9. Normalized EMG and motor unit (MU) amplitude [mean (SD)] for vastus medialis  
558 (VM, white dots) and vastus lateralis (VL, black dots) at 10, 30, 50 and 70% of the maximum  
559 voluntary contraction torque (MVC). A) Normalized root mean square EMG (EMG RMS  
560 NORM), B) Normalized MU root mean square (MURMS NORM). # Main effect of muscle  
561  $P = 0.039$ .

562

563

564

565

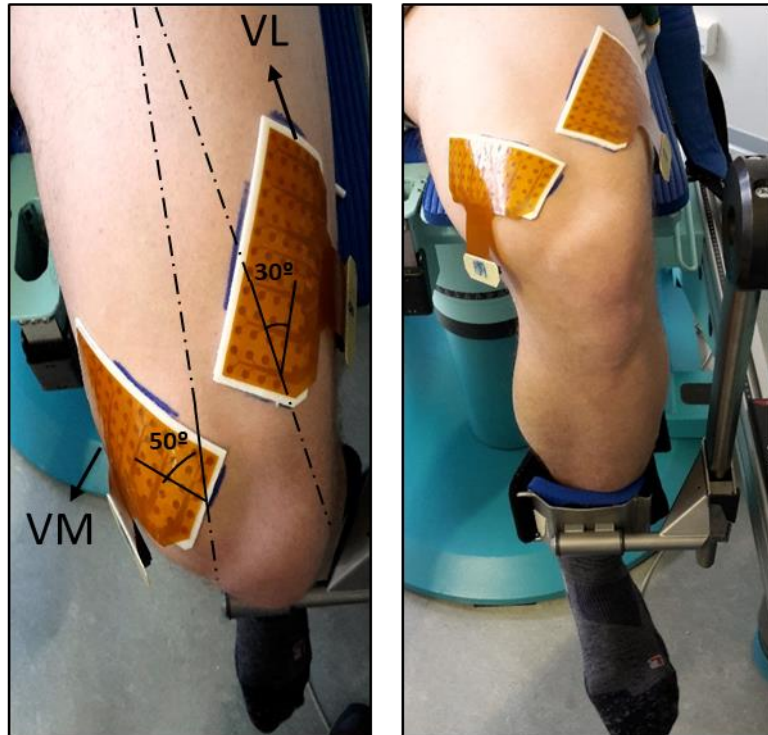
566

567

568

569





570  
571 Figure 1

572

573

574

575

576

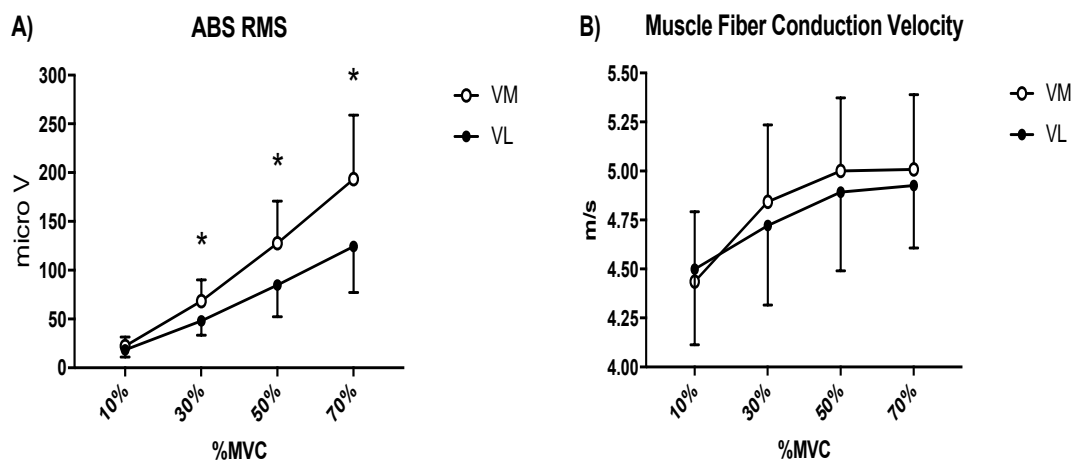
577

578

579

580

581



582 Figure 2

583

584

585

586

587

588

589

590

591  
592  
593  
594  
595  
596  
597  
598  
599  
600

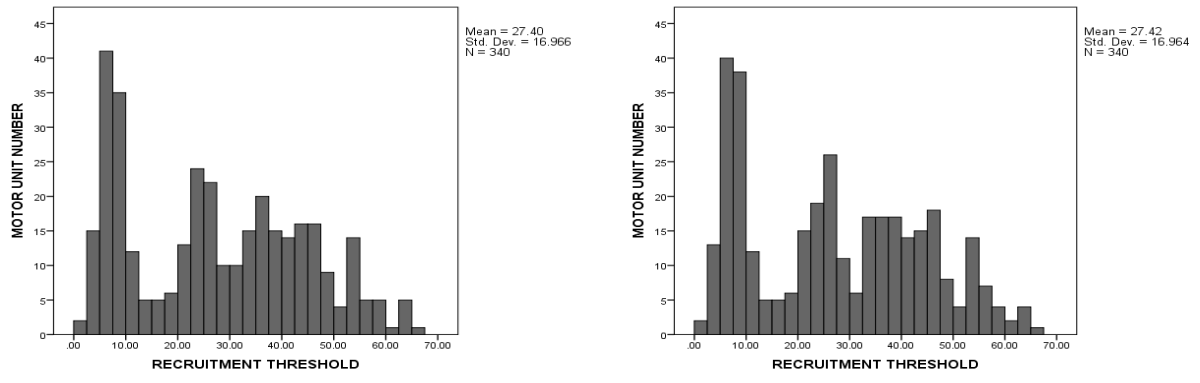
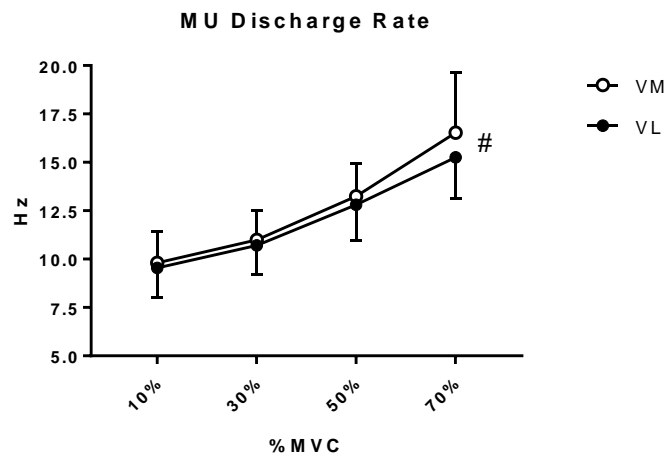


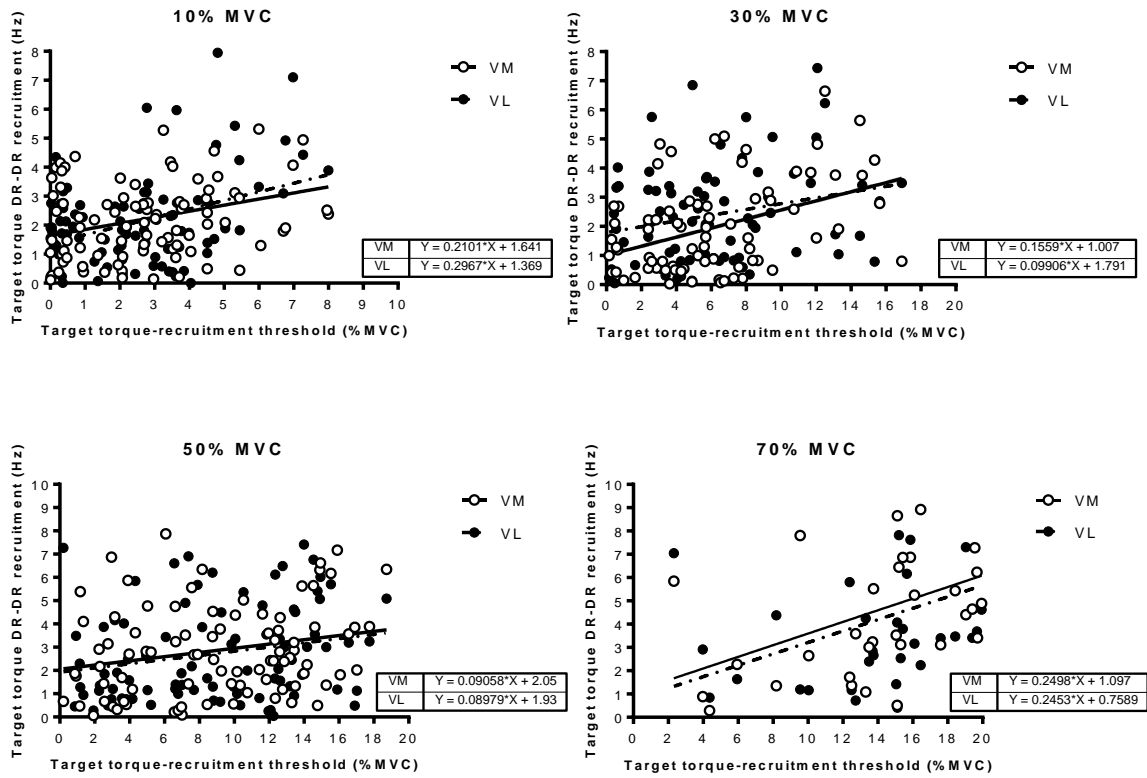
Figure 3



601  
602

Figure 4

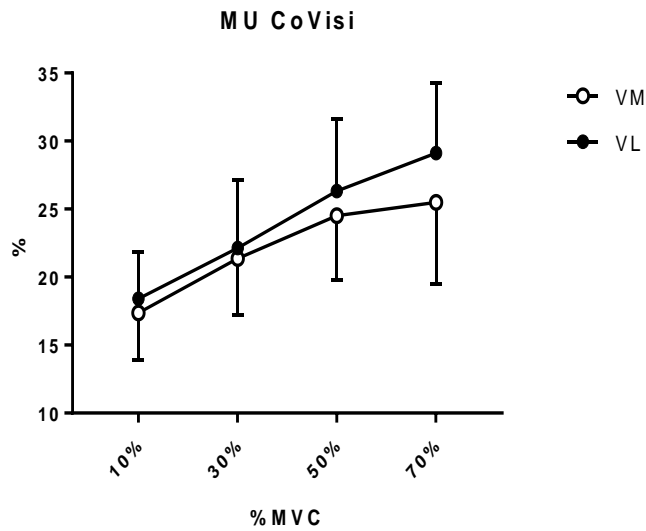
▲ Discharge rate vs. ▲ Recruitment



603

604 Figure 5

605



606

607 Figure 6

608

609

610

611  
612  
613  
614  
615  
616  
617  
618  
619  
620  
621  
622

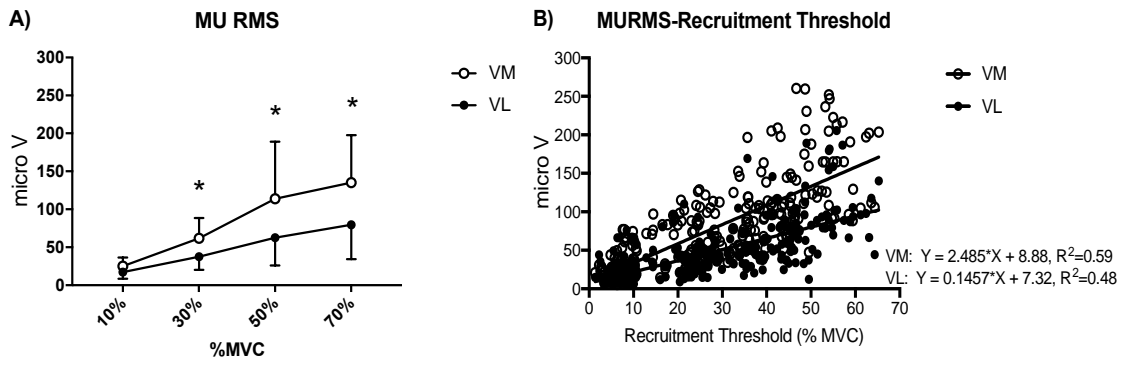
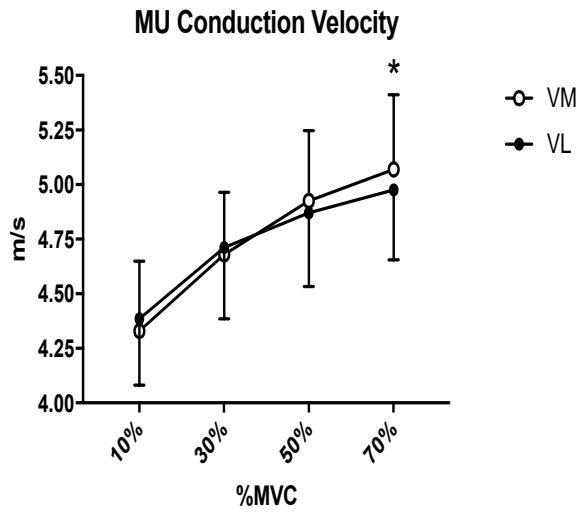
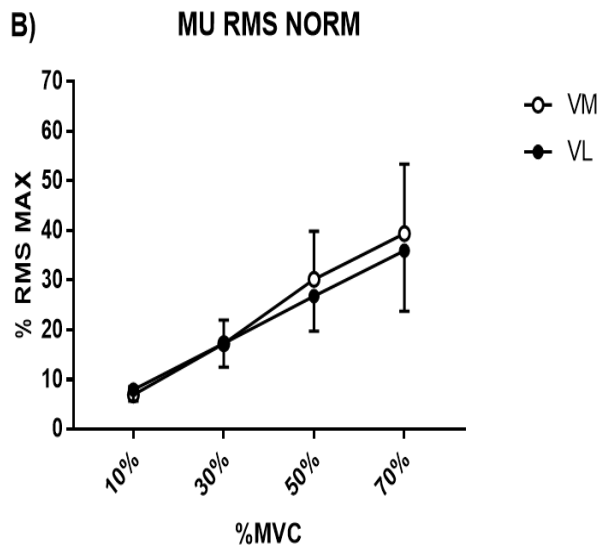
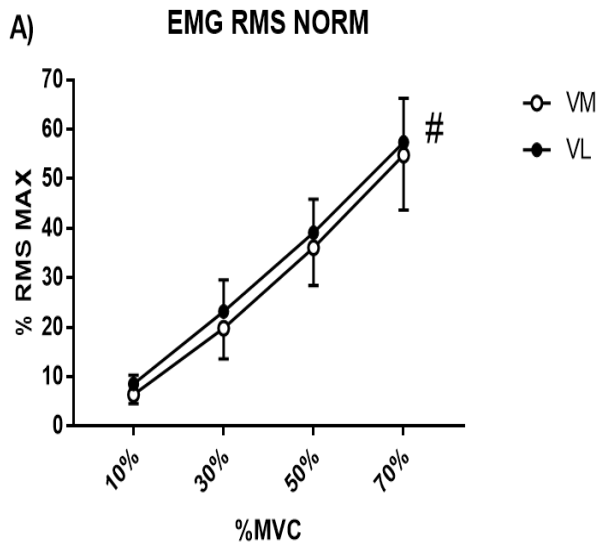


Figure 7



623  
624  
625  
626

Figure 8



627  
628 Figure 9